International Civil Aviation Organization

The Twenty-First Meeting of the Regional Airspace Safety Monitoring Advisory Group (RASMAG/21)

Bangkok, Thailand, 14-17 June 2016

Agenda Item 5: Airspace Safety Monitoring Activities/Requirements in the Asia/Pacific Region

VERTICAL OVERLAP PROBABILITY PARAMETER RE-ESTIMATION

(Presented by the United States/PARMO)

SUMMARY

The current estimate of the probability of vertical overlap for use in the Pacific vertical collision risk model was developed prior to the implementation of the RVSM in calendar year 2000. This paper develops an updated estimate of the vertical overlap probability based on recent estimates of the aircraft population, reports of large height deviations which were found to be unrelated to operational causes, aircraft height-keeping performance data, and altitude deviation data.

1. INTRODUCTION

1.1 The assessment of vertical risk is divided into two major parts – technical and operational. The estimate of technical risk in Pacific airspace is significantly below the Target Level of Safety (TLS). The low level of technical risk has been attributed to the successful application of the Minimum Aircraft System Performance Specification (MASPS) used in combination with identifying and resolving problems uncovered during monitoring.

1.2 The last estimate of the probability of vertical overlap for Pacific airspace was completed as part of the implementation of the RVSM in calendar year 2000. The current parameter value for the vertical overlap probability, defined as the probability that two aircraft which are nominally separated by the vertical separation minimum are in vertical overlap, used in the Pacific vertical risk collision risk estimate was estimated as 2.46×10^{-8}. This value depends on the development of the Total Vertical Error (TVE) distribution, with component elements, Altimetry System Error (ASE) and Assigned Altitude Deviation (AAD) distributions.

1.3 The purpose of this paper is to develop an updated estimate for this vertical overlap probability based on recent estimates of the aircraft population, reports of large height deviations which were found to be unrelated to operational causes, aircraft height-keeping performance data, and altitude deviation data.

2. DISCUSSION

2.1 The December 2015 traffic sample data (TSD) was used to provide information on the aircraft types employed in the airspace. Figure 1 presents the distribution of observed aircraft types from the TSD. The top 25 aircraft types in terms of flying hours shown in Figure 1 represent approximately 96 percent of all the aircraft types observed in the data sample.

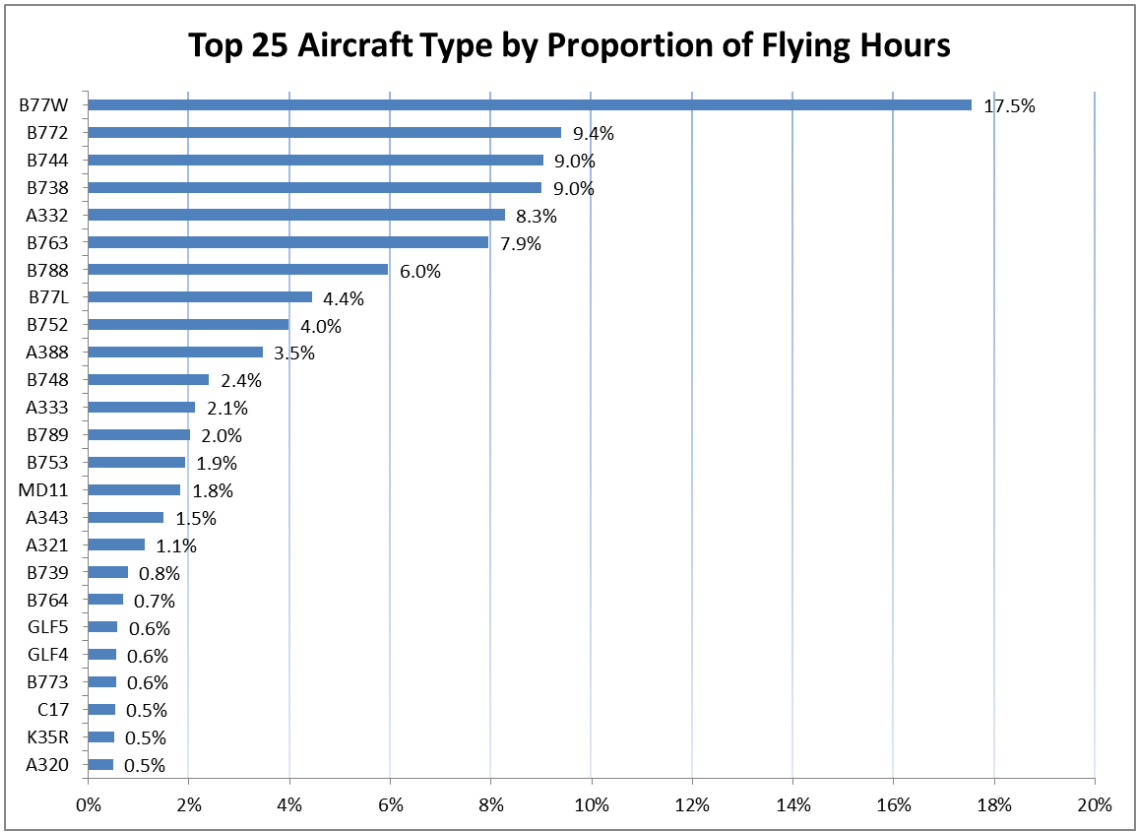

Figure 1. Top 25 Aircraft Types Observed by Proportion of Flying Hours

2.2 Figure 1 shows the most frequently observed aircraft type is the Boeing 777-300ER (B77W) aircraft. The top five aircraft types in terms of number of operations account for more than 53 percent of all the flying hours by aircraft type in the TSD.

2.3 Estimates of the probability of vertical overlap, $P_z(1000)$, due to Altimetry System Error (ASE) and altitude-keeping deviations are based on statistical distribution modeling. The same procedures developed and used to estimate the initial vertical overlap probability for Pacific airspace used in this work. These procedures are described in detail in reference 1.

2.4 The statistical distribution of altitude-keeping deviations is estimated in a three step process. The first step includes collecting mode C (or mode S) altitude, constructing a histogram of assigned altitude deviation (AAD) and fitting it to a distribution model for an estimate of typical performance. The second step in estimating the distribution for altitude-keeping deviations includes combining the modeled typical performance with large-height deviations reports collected in the airspace. The third and final step in estimating the distribution for altitude-keeping deviations is to fit a statistical distribution model to the combined typical performance and large-height deviations.

2.5 An estimate of the distribution of ASE is also constructed in three parts. First, weighted estimates of the means and standard deviations of ASE for each aircraft type are computed from the aircraft ASE data. The weights are based on the estimated number of flying hours observed in the airspace for each aircraft type. Second, an ASE distributional form is chosen for each aircraft type observed in the airspace. Lastly, the proportion of time that each aircraft type is observed in Pacific RVSM airspace is used to combine the ASE distributions by aircraft group into an ASE distribution representative of the airspace.

2.6 Under the assumption that the components of ASE and altitude-keeping are independent, the distributions are statistically combined to construct an estimate of the distribution of TVE. Then

based on the average Pacific airspace aircraft height, the probability that two aircraft lose all vertical separation, $P_z(1000)$, is computed.

2.7 Estimation of Flight Technical Error

2.8 The AAD data are used as a surrogate to estimate the Flight Technical Error (FTE) distribution. The AAD data are derived from a radar data set. The raw radar data are recorded and extracted to text files using software developed by the 84th Radar Evaluation Squadron (RADES) of the United States Air Force (USAF) which allows for data filtering. Filters are set to extract the following from the raw data; beacon reinforced messages, Mode C values between FL290 and FL410, and traffic within preset geographic boundaries. The RADES software contains a graphical viewer with an option to output the data in ASCII format. The output file contains a version of the original data reduced according to the filters selected before running the software.

2.9 It is difficult to obtain radar data from enroute aircraft operations within oceanic airspace. However, radar data from the Bermuda area in the Atlantic Ocean was made available for this work. A sample radar image, showing the geographical area represented from the Bermuda radar taken with the RADES software is shown in Figure 2. The data displayed in Figure 2 represent one day in March 2010 of flight data from the Bermuda radar. The data in the Bermuda radar coverage area were filtered to include aircraft operating in the east/west direction, as these aircraft operations include more commercial aircraft types compared to the aircraft types operating in the north/south direction.

2.10 The level flight portions of the data collected over Bermuda are used in this analysis. Sixty-two days of AAD data were collected with a total flying time of 3,618.91 hours. The AAD sample mean and sample standard deviation were computed to be 0.0055 ft and 19.05 ft, respectively.

Figure 2. Sample Radar Image Showing Operations from the Bermuda Radar

2.11. The data collected from the Bermuda radar were modeled as a mixture distribution consisting of a Gaussian core and a Double Exponential tail distribution. Once typical performance is estimated, relative frequencies for each 100-ft class interval of the mixture of a normal core and Double Exponential tail distributions are computed. The parameter values for the AAD distribution model are given in Table 1. The density form for this distribution is given in equation 1.

$$f(z;\sigma,\lambda,\alpha) = \frac{(1-\alpha)}{\sqrt{2\pi\sigma}} e^{-\frac{z^2}{2\sigma^2}} + \frac{\alpha}{2\lambda} e^{-\frac{|z|}{\lambda}} \quad (1)$$

2.12. The density in equation 1 is a weighted sum of a Gaussian density and a Double Exponential density, the Gaussian portion is referred to as the "core" density and the Double Exponential portion is referred to as the "tail" density. The portion of equation (1) which represents the Gaussian core is $\frac{(1-\alpha)}{\sqrt{2\pi\sigma}} e^{-\frac{z^2}{2\sigma^2}}$ and the portion of equation (1) which represents the Double Exponential tail is $\frac{\alpha}{2\lambda} e^{-\frac{|z|}{\lambda}}$. The mixing parameter, α, provides the 'weights' to the core and tail portions of the distribution and is estimated for each case presented in Table 1. The estimates for the standard deviation parameter, σ, for the Gaussian portion, and the rate parameter, λ, for the Double Exponential distribution are in Table 1.

Table 1: Distribution Modeled to AAD data

Data Source	Sample Statistics	Model	Parameters
AAD Distribution – Bermuda Radar	Mean = 0.005 ft SD = 19.046 ft	Mixture of Normal (core) and 1st-Laplace (tail)	σ = 22.977 λ = 54.771 α = 0.0106

2.13. The results shown in Table 1 show that the contribution from the core portion of the density function dominates the distribution fit for the AAD data. The choice in using a mixture distribution to model the AAD data differs from that previously chosen in reference 1. In reference 1 a single distribution form, the Double Exponential distribution was chosen to model the AAD data. The corresponding $P_z(0)$ and $P_z(1000)$ values for the modeled AAD distribution are 0.887 and 3.195×10^{-10}, respectively.

2.14. Estimation of AAD and Large Height Deviation Data Distribution

2.15. To account for the influence of turbulence and other large height deviations (related to technical risk) on the estimate of $P_z(1000)$, reports of risk bearing deviations are used. Reports from the North Atlantic (NAT) airspace provided by the Central Monitoring Agency (CMA) were used in this analysis. The reports of turbulence and other large height deviations were for the three-year period of January 2007 through December 2009. These reports were considered to be attributable to technical and not operational risk.

2.16. During the three-year period from January 2007 through December 2009, there were **31.7 minutes** of flying time during which large height deviations attributable to technical risk occurred. These data were added to the AAD data. Table 2 provides the details of the each large height deviation report included in this work. Some of the events listed in Table 2 resulted in the aircraft being re-cleared to a new flight level. For these instances a standard value was applied in the maximum height deviation and total duration, an asterisk, "*" indicates these cases. The standard value applied to these cases was taken to be the average absolute value of the maximum height deviation and duration for the remaining technical events.

Table 2. Reported Large Height Deviations Attributable to Technical Risk in the NAT During the Time Period of January 2007 and December 2009

Date	Aircraft Type	Direction	Height Dev(+/- feet)	Total Duration (min)	Cause of deviation
17-Jan-2007	B772	W	700	2	Turbulence

Date	Aircraft Type	Direction	Height Dev(+/- feet)	Total Duration (min)	Cause of deviation
1-Oct-2007	B741	E	-400	2	Ambient temperature
21-Oct-2007	B738	E	600*	1.65*	Turbulence
2-Nov-2007	A332	W	500	2	Turbulence
2-Dec-2007	B744	E	300	5	Turbulence
19-Dec-2007	B773	E	-750	2	Turbulence
2-Feb-2008	A332	W	600*	1.65*	Turbulence
28-Feb-2008	A332	E	400	2	Turbulence
30-Aug-2008	B744	E	400	2	Turbulence
2-Sep-2008	A332	E	-500	1	Turbulence
24-Nov-2008	C510	W	-700	0.5	Autopilot malfunction
21-Feb-2009	A332	E	-1100	1	Turbulence
12-Jun-2009	F900	W	-500	1	Ambient temperature
12-Jun-2009	B772	W	300	0.5	Turbulence
18-Jun-2009	GLF4	E	500	1	Turbulence
18-Sep-2009	GLF4	W	-420	1	Turbulence
19-Oct-2009	B772	E	-600*	1.65*	Turbulence
21-Oct-2009	CL60	W	-400	0.75	Ambient temperature
15-Nov-2009	VC10	E	800	1	Autopilot malfunction
11-Dec-2009	B744	E	800	1	Turbulence
31-Dec-2009	A320	E	1300	1	Windshear

2.17. Combining the AAD data with the large height deviation data is accomplished by first creating a relative histogram for the AAD data. The relative histogram for the AAD data is then adjusted for the amount of flying hours over the time period which the large height deviation data were collected. In this work, the large height deviation data were collected over a time period of three years, with 1,365,000 annual flying hours per year. The time-adjusted AAD histogram is then combined with the large height deviation data and fit to a statistical distribution.

2.18. The best fit for the AAD resulted in a mixture of two distributions as shown in Table 1. Therefore, the addition of the reported large height deviations attributed to technical risk required a mixture of three distributions to properly model the combined AAD and large height deviation data. This modeled distributional fit accommodates the mixture distribution in the AAD data and the added distribution of the large height deviation data. The corresponding $P_z(0)$ and $P_z(1000)$ values for the AAD and large height deviation data are 0.887 and 3.264×10^{-10}, respectively.

2.19. *Estimation of the ASE Distribution*

2.19.1. The ASE data used in this analysis were obtained from the FAA's Aircraft Geometric Height Monitoring Element (AGHME) system during the time period of January 2015 through April 2016.

2.19.2. Reference 1 provides guidance in selecting statistical distributions to model the ASE for the aircraft groups. The data for each aircraft group or type are analysed by examining the distribution of ASE for two components. One component consists of the variation among the airframe ASE means, and the other component consists of the ASE variation within each airframe. The first component is constructed by computing the difference between the ASE mean of the aircraft group and the ASE mean of each airframe within the group. The second component is constructed by computing the difference between the ASE mean of each airframe and the ASE measurements of the corresponding airframe.

2.19.3. Table 3 provides the top twenty aircraft types, in terms of flying hours, for Pacific RVSM airspace. Together, these twenty aircraft types represent more than 94 percent of the flying hours in the airspace. Table 3 presents the corresponding ASE means, standard deviation, and proportion of flying hours. The Double Exponential distribution was chosen to represent the ASE performance for all aircraft types except for the A388. Based on the observed ASE data for the A388, the Normal distribution provided the best fit and was the choice to represent the ASE performance for this aircraft type. The modeled ASE performance by aircraft type for approved operations is shown in Figure 3 for the top 10 aircraft types.

Table 3. 2015 Observed Aircraft Types in Pacific RVSM Airspace

Aircraft Type	Proportion Flying Time	ASE Mean (ft)	ASE St Dev (ft)
B77W	17.54%	34.954	49.111
B772	9.39%	13.688	51.894
B744	9.03%	-88.523	52.647
B738	9.00%	1.981	52.246
A332	8.27%	30.609	55.223
B763	7.95%	-63.482	65.324
B788	5.96%	35.934	44.988
B77L	4.45%	13.688	51.894
B752	3.98%	-33.861	66.720
A388	3.46%	-29.43	49.171
B748	2.40%	16.944	45.808
A333	2.12%	30.609	55.223
B789	2.02%	35.934	44.988
B753	1.92%	-24.858	57.918
MD11	1.83%	0.510	66.994
A343	1.50%	7.237	46.397
A321	1.12%	33.246	66.594
B739	0.79%	1.981	52.246
B764	0.69%	-17.740	67.016
GLF5	0.58%	37.802	74.027
	94.01%		

2.19.4. The distribution of ASE for the airspace is estimated by constructing a weighted sum of statistical distribution models for different aircraft groups/types. The proportion of total flight time each aircraft group is used to construct the “weights” for each aircraft group. ASE means and standard deviations (used to derive the parameters for the statistical distribution models) of each aircraft group are estimated directly from the ASE data -- after taking into consideration the different

number of ASE measurements for each airframe monitored and removing the estimate of measurement system error.

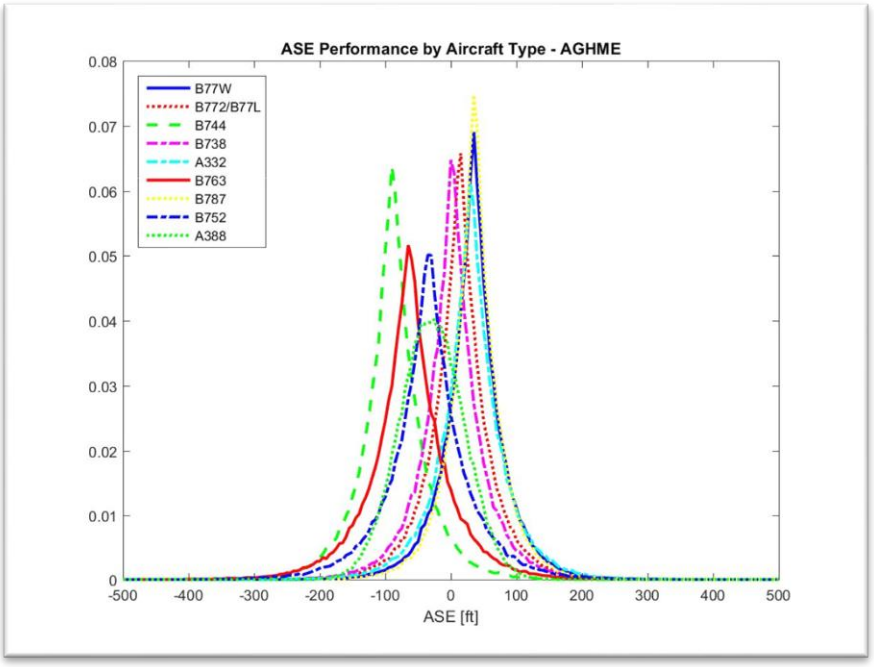

Figure 3. Modeled ASE Performance by Aircraft Type

2.20. Estimation of Vertical Overlap Probability for Pacific Airspace

2.20.1. After the ASE distributions for each aircraft group were mixed in the proportions shown within Table 3 and then statistically combined with the AAD data and large height deviation distribution, the resulting TVE distributions were used to compute estimates of the probability of vertical overlap. Table 4 shows the vertical overlap probability estimates as each data set are added.

Table 4. Probability of Vertical Overlap

Data Source	$P_z(0)$	$P_z(1000)$
AAD Data	0.887	0.319×10^{-9}
AAD and Large Height Deviation Data	0.887	0.326×10^{-9}
AAD, Large Height Deviations, and ASE Data Combined	0.420	4.682×10^{-9}

2.20.2. Table 4 shows the $P_z(0)$ and $P_z(1000)$ estimates for the Pacific RVSM airspace. The first row of estimates includes the AAD data only. The second row of estimates includes the AAD combined with all large height deviations attributable to technical risk. The third row includes the ASE data combined with AAD and large height deviation data. All vertical overlap probabilities were computed with an assumed average aircraft height of 53-ft.

2.20.3. The current estimate of the probability that two aircraft which are nominally separated by 1000 ft are in vertical overlap, *Pz(1000)*, for the Pacific is 2.46×10^{-8}. The estimate for this probability provided in this paper, 4.682×10^{-9}, is lower than the current estimate. The next section provides some comparative analyses between the previous estimate of vertical overlap probability and the current estimate.

2.21. Comparison of current and previous estimates of vertical overlap probabilty

2.21.1. Figure 4 illustrates the difference between the current estimate of vertical overlap probability and the updated estimate provided in this paper.

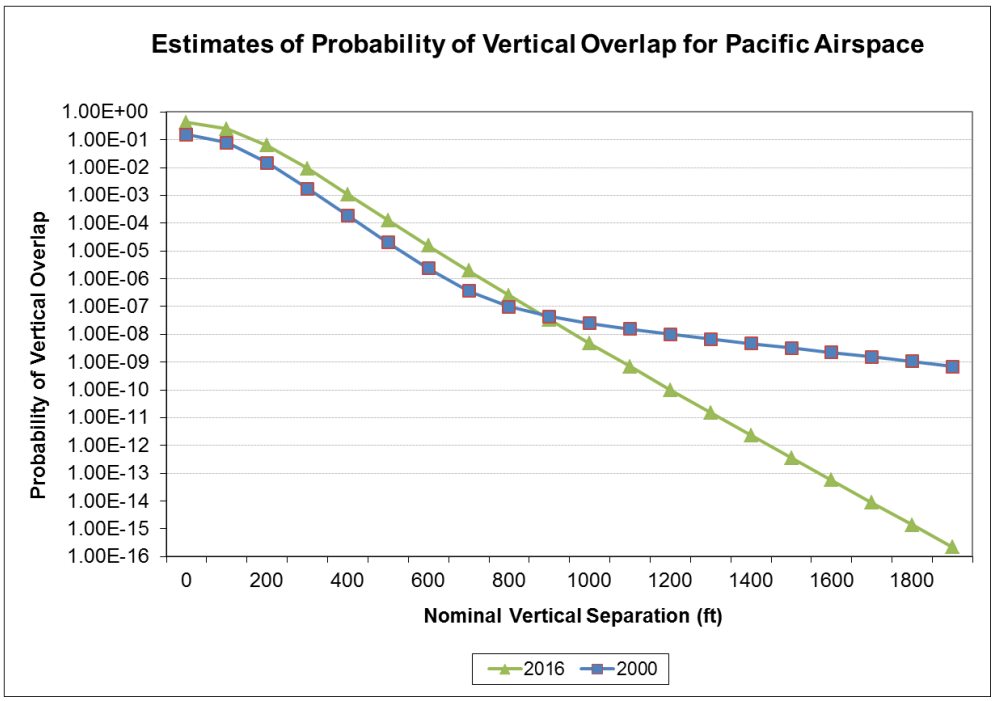

Figure 4. Comparison of Current to Previous Estimates

2.21.2. To further illustrate the differences between the two estimates, the previous data used to model the ASE performance in the airspace is compared to more recent data. Figure 5 contains the resulting probability of overlap using the different sets of AAD and LHD data with the old and new ASE data.

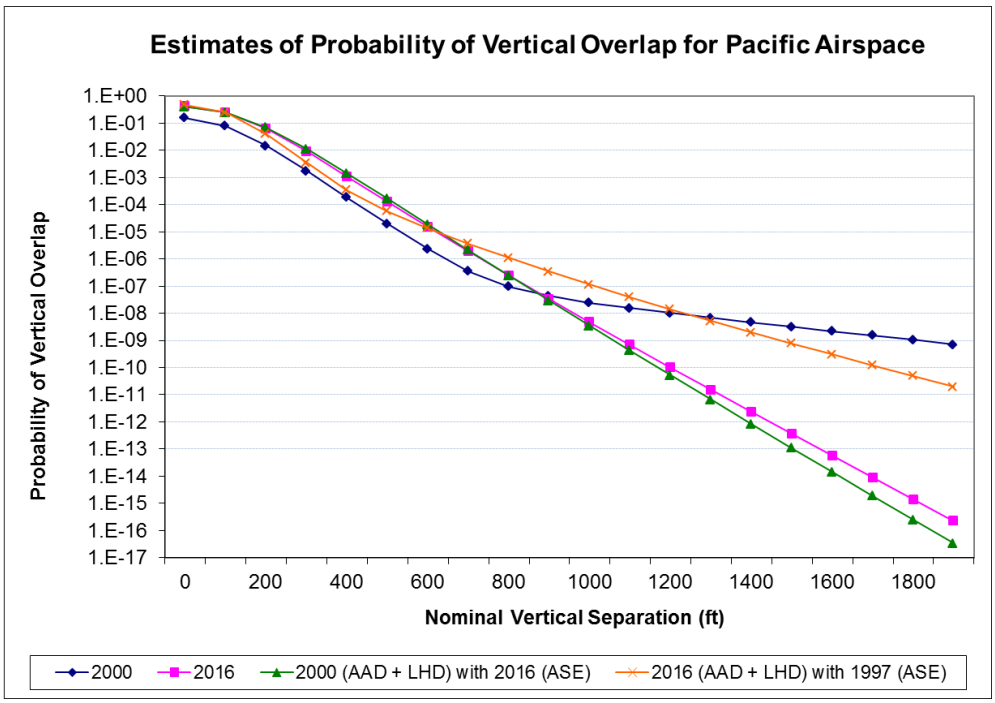

Figure 5. Comparison of Estimates by Current and Previous Data Sets

2.21.3. Based on the information presented in Figures 4 and 5, most of the difference between the current and updated estimates can be attributed to the ASE data. The year 2000 ASE data set consisted of older aircraft types. Figure 6 provides a similar plot as contained in Figure 3 for the older ASE data available in calendar year 2000.

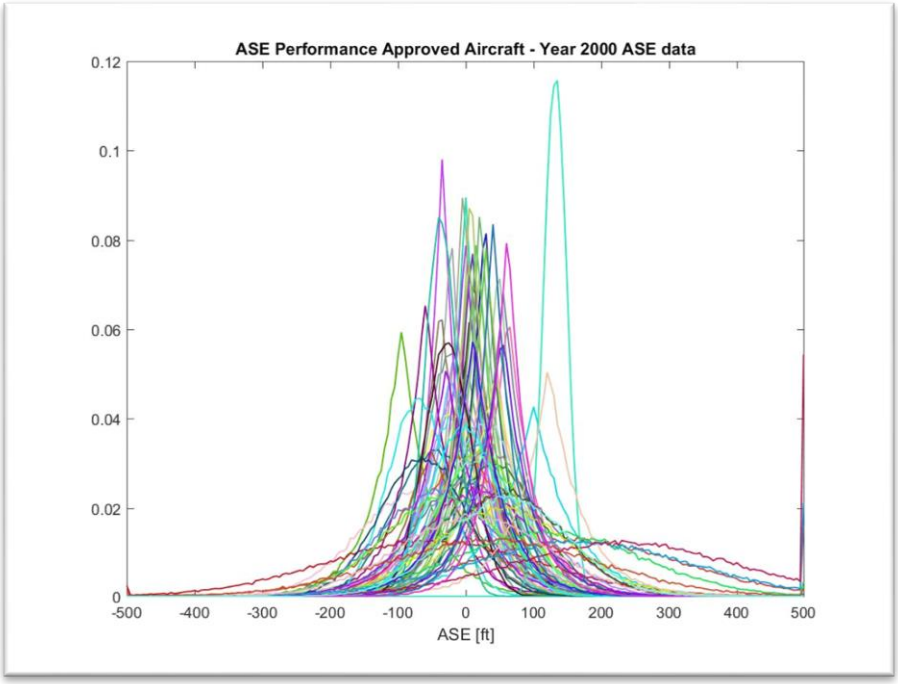

Figure 6. Modeled ASE Performance by Aircraft Type/Group – Calendar Year 2000 Data

2.21.4. Figure 6 shows more varied performance levels of aircraft ASE in the data set from calendar year 2000. It is noted that the availability of aircraft ASE data was limited in calendar year 2000 compared to today. The primarily source for data were the GPS Monitoring Unit (GMU) and the Height Monitoring Units (HMUs) in the North Atlantic.

2.21.5. The 2000 data set contained 104.75 minutes of large height deviations, these deviations were collected over a one year period. The more recent data set contained 30.7 minutes of large height deviations which were collected over a three year period. The largest deviation in the 2000 data set accounted for 43 minutes of flying time. The maximum deviation in terms of distance from cleared flight level was 1200 ft with a corresponding time of 6 minutes in the 2000 LHD data. The maximum deviation in terms of distance from cleared flight level was -1100 ft with a corresponding time of one minute in the more recent LHD data.

3. ACTION BY THE MEETING

3.1 The meeting is invited to:

a) note the information contained in this paper; and

b) discuss any relevant matters as appropriate.

…….

References

1. "Summary of Statistical Distributions Modeled to Aircraft Altitude-Keeping Deviations and Altimetry System Errors and the Resulting Estimate of the Probability of Vertical Overlap for NAT RVSM", NAT SPG/34 MWG IP/8, Brussels, 2-5 June 1998.